

有机纳米光学传感器及血糖定量成像研究

刘静^{1,2}, 房晓峰², 袁振¹, 吴长锋^{2*}¹澳门大学健康科学学院癌症研究中心, 澳门 999078;²南方科技大学工学院生物医学工程系, 广东 深圳 518055

摘要 连续血糖监测是糖尿病预防、诊断及管理过程中的有效手段。然而,现有的电化学连续血糖监测系统仍存在开放式创口植入、易引起炎症、监测时间短等缺点。光学传感为连续血糖监测提供了新方法,本团队设计开发了可见光激发的发光纳米粒子葡萄糖传感器,其高亮度的发光传感特性有助于经皮血糖信号检测。基于比率荧光策略设计的发光纳米粒子可以校准激发光强变化和采样环境变化等带来的信号误差,可见光激发发光特性可以避免紫外光激发采样对机体的伤害,在高频率长时段的信号采集应用中具有明显优势。

关键词 生物医学; 传感器; 纳米传感器; 生物传感器; 血糖监测

中图分类号 R318

文献标志码 A

DOI: 10.3788/CJL202249.1507403

1 引言

糖尿病是一种慢性非传染性疾病,其并发症可累及心脏、肾脏、神经系统及泌尿系统等^[1],不断攀升的糖尿病发病率及其并发症已给社会造成极大的医疗经济负担^[2]。有效的血糖监测可以提供即时的血糖信息,是糖尿病预防、诊断及管理过程中的重要手段^[3]。相较于单点血糖信息测试,连续血糖监测系统可以通过高频检测追踪血糖信息的波动情况,有助于预测血糖的走势^[4]。在以往的研究中,电化学血糖测试系统通过植入型微电极采集皮下组织液中的血糖信息,然后通过与其连接的信号传输装置,将血糖信息转译成电信号并传输保存至终端,但经皮植入电极的方式会造成开放型创口且存在易感染的风险^[5-7]。微透析系统通过组织液透析的方式持续采集微量组织液并离体测试血糖浓度,可以得到持续的血糖信息^[8]。光学成像以其特有的信号传输方式,可以构建完全植入型传感器,实现血糖信息的连续经皮探测和传输,避免了上述植入方式的风险^[9-14]。

有机发光纳米粒子以其高发光亮度、高光稳定性及良好的生物相容性,在生物成像、生物传感、疾病诊断及治疗等领域具有广阔的应用前景^[15-18]。在前期工作中,本团队基于半导体聚合物构建了高亮度的发光纳米粒子,将其偶联耗氧酶实现了对葡萄糖小分子的灵敏检测,并实现了植入机体后长时间稳定传感^[19]。进一步,本团队通过筛选具有不同磷光寿命的氧敏感染料,构建了超高灵敏度的葡萄糖传感器;同时构建了

与之适配的微型智能手机检测系统,实现了无线连续血糖监测,并且可以通过手机采集皮下植入传感器的图像,对图像进行处理分析后即可识别高血糖与正常血糖状态^[20-22]。然而,在前期实验中使用的共轭聚合物纳米颗粒通常采用紫外光作为激发光源,在血糖检测的同时可能会对机体造成损伤,从而限制了该传感器在高频率长时段连续血糖监测中的应用^[23]。鉴于此,本团队通过筛选荧光小分子与长磷光寿命的氧敏感染料,设计并制备了由可见光激发的发光纳米粒子;然后利用上述两种染料制备了稳定的具有氧敏感特性的发光纳米粒子,并将耗氧的葡萄糖氧化酶修饰于发光纳米粒子表面,构建具有葡萄糖传感特性的光学传感器。荧光光谱测试结果表明该传感器具有高检测灵敏度以及对不同浓度葡萄糖的快速响应能力。本团队进一步对该传感器进行了细胞内葡萄糖浓度检测以及在体皮下血糖浓度检测,检测结果表明,该传感器可为发展高频率长时段连续血糖检测提供有益参考。

2 实验部分

2.1 实验材料

2,2'-(1-(3-methoxyphenyl)-2-(4-methoxyphenyl)ethene-1,2-diyl) bis(9,9-dimethyl-9H-fluorene) (DPBF) 荧光小分子合成路径见参考文献^[24]。磷光染料钯(II) meso-四(五氟苯)卟啉(PdTFPP)购自 Frontier Scientific 试剂公司。两亲性聚合物聚苯乙烯马来酸酐(PSMA, 异丙基苯终端,平均相对分子质量为 1700)、四氢呋喃

收稿日期: 2021-11-25; 修回日期: 2021-12-28; 录用日期: 2022-01-19

基金项目: 国家自然科学基金(81771930)、国家重点研发计划(2020YFA0909000)、深圳科技计划项目(KQTD20170810111314625, JCYJ20210324115807021)、深圳湾实验室资助项目(SZBL2021080601002)

通信作者: *wucf@sustech.edu.cn

(THF)、葡萄糖氧化酶(GOx)、葡萄糖、磷酸盐缓冲溶液(PBS 缓冲液)、二甲基亚砜(DMSO)均购自 Sigma-Aldrich 试剂公司。1-(3-二甲氨基丙基)-3-乙基碳二亚胺盐酸盐(EDC)购自 J&K 试剂公司。羟乙基哌嗪乙硫磺酸溶液(HEPES 缓冲液)购自康宁公司。人类乳腺癌细胞(MCF-7)购自中国科学院细胞库。细胞培养基(DMEM)、无糖细胞培养基、胎牛血清(FBS)、双抗生素、胰蛋白酶均购自 Hyclone 试剂公司。3-(4,5-二甲基噻唑-2)-2,5-二苯基四氮唑溴盐(MTT)购自 Promega 公司。

2.2 仪器表征

采用 Shimadzu UV-2550 紫外可见吸收光谱仪和 Hitachi 4600 荧光光谱仪测试表征纳米颗粒的光谱特性。采用 Malvern Nano ZS 动态光散射粒度仪测试表征生物偶联前后纳米颗粒的水合动力学直径和表面电位。采用 Hitachi HT7700 透射电子显微镜(TEM)测试表征纳米颗粒的形貌。采用 SYNERGY-H1 酶标仪测定 490 nm 和 570 nm 处的吸光度,以测定材料的细胞毒性。采用 DMI6000B 倒置荧光显微镜采集细胞的发光图像。采用 IVIS Spectrum 可见光小动物活体光学成像系统采集动物实验的发光图像,激发波长为 520 nm,采集波长为 670 nm。

2.3 有机纳米光学传感器的制备

采用再沉淀法制备具有氧敏感特性的发光纳米材料^[25-26]。首先将 DPBF 荧光小分子、磷光染料 PdTFPP 及两亲性聚合物 PSMA 分别溶解于 THF 中,制得 1 mg/mL 的原始溶液;然后用 THF 按比例将三种原始溶液稀释,得到用于制备发光纳米粒子的前驱混合溶液(前驱混合溶液中 DPBF 的质量浓度为 100 $\mu\text{g}/\text{mL}$, PdTFPP 的质量浓度为 10 $\mu\text{g}/\text{mL}$, PSMA 的质量浓度为 150 $\mu\text{g}/\text{mL}$);随后,将 10 mL 超纯水置于超声水浴锅中,然后将 2 mL 充分混合均匀的前驱溶液垂直悬于超纯水液面上,并快速注入,持续超声 90 s;在氮气保护下,通过加热的方式将溶液中的 THF 组分去除,将溶液浓缩至所需浓度,即可制备得到氧敏感的发光纳米粒子 DPBF-PdTFPP-PSMA(以下简称为“DPP”)。

通过 EDC 催化作用下的酰胺反应进行生物偶联,将葡萄糖氧化酶修饰于发光纳米粒子表面。首先取 4 mL 发光纳米粒子水溶液(DPP 质量浓度为 50 $\mu\text{g}/\text{mL}$),加入 HEPES 缓冲溶液(80 μL , 1 mol/L, pH 为 6.5),以调节反应体系的 pH,接着相继加入葡萄糖氧化酶溶液(100 μL , 10 $\mu\text{mol}/\text{L}$, 溶解于 20 mmol/L HEPES 缓冲溶液中)和 EDC 溶液(80 μL , 5 mg/mL, 溶解于超纯水中,现用现配),在室温条件下持续搅拌混匀,反应 4 h 后得到具有葡萄糖敏感特性的有机纳米光学传感器 DPP-GOx。

2.4 有机纳米光学传感器的材料表征

使用紫外可见吸收光谱仪测试表征 DPBF 荧光小分子、磷光染料 PdTFPP 以及制备的氧敏感的 DPP 发光纳米粒子的吸收谱线。将 10 mg/mL 的 DPP 水溶

液滴于铜网上,室温干燥后,使用透射电子显微镜(电压为 100 kV)测试 DPP 的形貌。使用动态光散射粒度仪对生物偶联前后的 DPP 发光纳米粒子以及 DPP-GOx 传感器的水合动力学直径、表面电位进行检测。使用荧光光谱仪对 DPP-GOx 的葡萄糖敏感特性进行测试表征。将 DPP-GOx 水溶液置于比色皿中,加入葡萄糖溶液(响应体系中葡萄糖的终浓度分别为 0、4、8、12、16、20 mmol/L),在 410 nm 可见光激发下连续监测 672 nm 处的发光强度变化;响应 10 min 后,测试并记录不同葡萄糖浓度下传感体系的发光光谱。

采用人类乳腺癌细胞(MCF-7)进行 DPP 发光纳米粒子的细胞毒性测试。将细胞铺于 96 孔板,细胞密度为 60000 cell/mL,每孔 100 μL 。待细胞培养 24 h 并铺满板底后,加入不同浓度的 DPP,共孵育 24 h。采用噻唑蓝(MTT)测试细胞活性。每孔加入 20 μL MTT 溶液(5 mg/mL 溶解于 PBS 缓冲液中),共孵育 3 h 后,吸去孔内液体,每孔加入 150 μL 二甲基亚砜(DMSO),并低速振荡 10 min,采用酶标仪测量每孔溶液在 490 nm 和 570 nm 下的吸光度,计算细胞毒性。

采用聚丙烯酰胺水凝胶作为载体测试该传感器葡萄糖响应的可重复性。将传感器包埋于聚丙烯酰胺水凝胶中,并将其依次置于 PBS 环境与葡萄糖溶液中,如此循环往复,测试传感器在 670 nm 处的发光强度。将该传感器置于过氧化氢(20 mmol/L)环境中,并采用手持式紫外灯(0.69 mW/cm²)进行紫外照射,测试不同照射时长后该传感器于 670 nm 处的发光强度。

2.5 细胞内葡萄糖水平的监测实验

采用人类乳腺癌细胞进行有机纳米光学传感器 DPP-GOx 对细胞内葡萄糖水平的监测实验。将细胞铺于玻璃底培养皿中,细胞密度为 60000 cell/mL,每皿 2 mL;待细胞培养 24 h 并铺满板底后,加入 DPP-GOx 传感器共孵育 12 h,在此期间使用无糖培养基进行细胞培养;向细胞培养基中引入葡萄糖溶液(葡萄糖的终浓度为 20 mmol/L)并采集细胞的发光图片(分别采集空白细胞组、与传感器共孵育但置于无糖培养基环境中的细胞组,以及与传感器共孵育并置于无糖培养基环境后引入葡萄糖溶液的细胞组的发光图片)。

2.6 活体动物体内葡萄糖监测实验

选用 8 周龄 Balb/c 小鼠(雌性,体重 25 g)进行活体动物体内葡萄糖监测实验,每组实验选用 3 只小鼠。选用异氟烷气体麻醉方式对小鼠实施麻醉。在小鼠麻醉的状态下,于其下背部皮下植入 50 μL DPP-GOx。采用可见光小动物活体光学成像系统采集小鼠的发光图像,激发波长为 520 nm,采集波长为 670 nm,曝光时间为 1 s。在实验中,通过腹腔注射葡萄糖溶液(1 mol/L,溶解于水中)的方式提高小鼠体内的血糖水平,采集小鼠尾部血液并采用商用血糖仪(Roche Accu-Chek)进行血糖检测,获取小鼠的血糖浓度值,并采集不同血糖浓度下的小鼠发光图像。在对照组中,于小鼠腹腔注射 PBS

后,采集小鼠的血糖信息以及对应的小鼠发光图像。

3 分析与讨论

3.1 有机纳米光学传感器的设计

本研究基于氧敏感的发光纳米粒子 DPP 构建具有葡萄糖传感特性的有机纳米光学传感器。首先选用可见光激发的 DPBF 荧光小分子、具有氧敏感特性的磷光染料 PdTFPP 及两亲性聚合物 PSMA,通过再沉淀法制备具有氧敏感特性的发光纳米粒子 DPP,如图 1 所示。在再沉淀过程中,两亲性材料 PSMA 中的马来酸酐单元水解形成羧基基团并分散于纳米材料表

面,同时将疏水性的磷光染料与荧光染料封装于发光纳米粒子内部,形成球形发光纳米粒子;进一步,通过生物偶联反应,将葡萄糖氧化酶修饰在粒子表面;在 EDC 的催化作用下,发光纳米粒子表面的羧基基团和葡萄糖氧化酶的氨基基团发生酰胺反应形成酰胺键,最终构建具有葡萄糖敏感特性的有机纳米光学传感器。当葡萄糖浓度发生变化时,由葡萄糖氧化酶引起的催化反应消耗纳米粒子环境中的氧气,将葡萄糖浓度的变化通过氧敏感的发光纳米粒子转化为发光信号强度。

光谱学测试结果显示发光纳米粒子 DPP 的主吸收峰位于 410 nm 处,如图 2(a) 所示,说明该粒子可

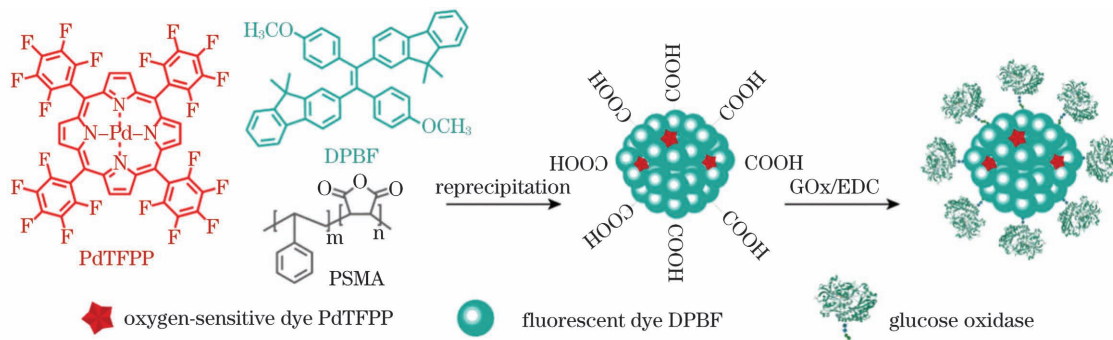


图 1 荧光小分子 DPBF、磷光染料 PdTFPP、功能化聚合物 PSMA 的分子结构式,以及有机纳米光学传感器的制备示意图(采用再沉淀法制备氧敏感的 DPP,然后将葡萄糖氧化酶修饰在 DPP 表面,构建有机纳米光学传感器 DPP-GOx)

Fig. 1 Molecular structures of fluorescent molecule DPBF, phosphorescent dye PdTFPP, and functional polymer PSMA, as well as preparation schematic of organic nanoparticle transducer (oxygen-responsive DPP was prepared via reprecipitation method, and then glucose oxidase was modified onto the surface of DPP to prepare organic nanoparticle transducer DPP-GOx)

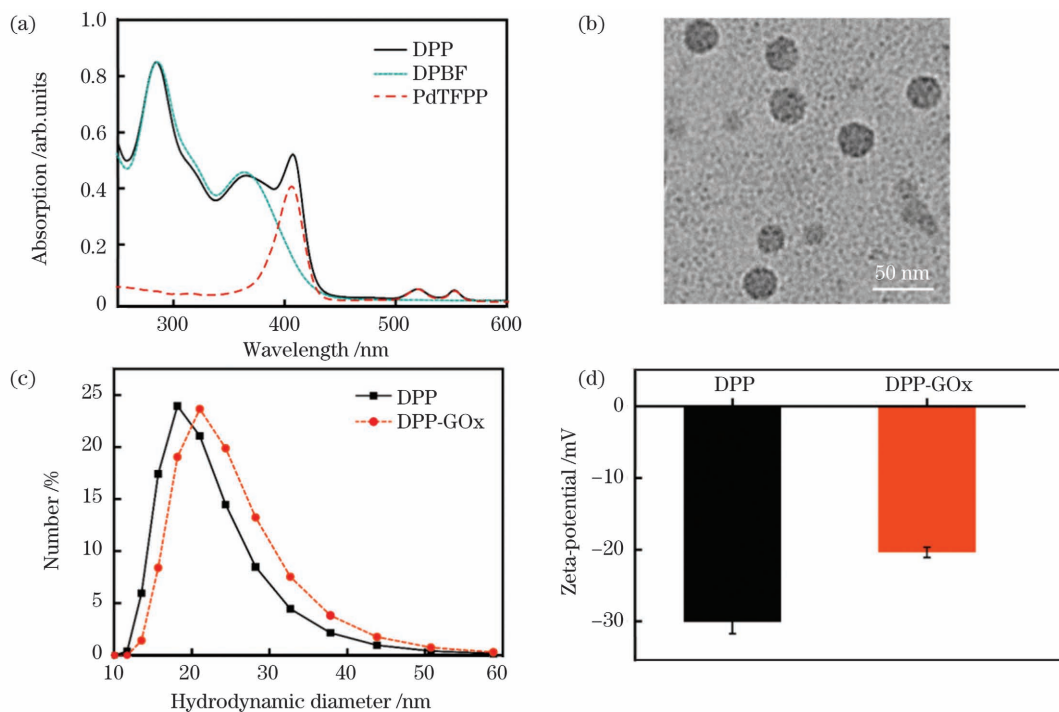


图 2 有机纳米光学传感器的表征。(a) 荧光小分子 DPBF、磷光染料 PdTFPP 及发光纳米粒子 DPP 的紫外可见吸收光谱;(b) 发光纳米粒子 DPP 的典型透射电子显微镜照片,图内标尺为 50 nm;(c) 进行生物偶联反应前后发光纳米粒子 DPP 的水动力学直径;(d) 进行生物偶联反应前后发光纳米粒子 DPP 的表面电位

Fig. 2 Characterization of organic nanoparticle transducer. (a) UV-Vis absorption spectra of fluorescent molecule DPBF, phosphorescent dye PdTFPP, and luminescent nanoparticle DPP; (b) representative TEM image of luminescent nanoparticle DPP, where the scale bar represents 50 nm; (c) hydrodynamic diameter of luminescent nanoparticle DPP before and after biological coupling reaction; (d) zeta-potential of luminescent nanoparticle DPP before and after biological coupling reaction

由可见光激发,避免了以往研究成像过程中紫外光激发对机体的伤害。透射电子显微镜图片显示纳米粒子 DPP 呈球形形貌,且具有单分散特性,如图 2(b)所示。该发光纳米粒子水溶液可稳定保存 30 d 以上,具有良好的胶体稳定性。生物偶联反应后,所制得的纳米粒子的水动力学直径由生物偶联反应前的 18 nm 增大到 21 nm,表面电位则由 -30 mV 增大至 -20 mV,证实了纳米粒子与葡萄糖氧化酶的偶联,如图 2(c)、(d)所示。所制备的发光纳米粒子葡萄糖传感器可用于后续体外传感测试、细胞内葡萄糖代谢成像测试及小鼠活体血糖成像测试。

3.2 有机纳米光学传感器的光谱学特性表征

光谱学测试结果显示该有机纳米光学传感器对生理范围的葡萄糖浓度检测具有高灵敏度、快速响应的特点。如图 3(a)所示,该有机纳米光学传感器在 490 nm 处有一个来自 DPBF 荧光小分子的荧光发射带,该信号强度不随葡萄糖浓度变化,可作为参比峰,用于实际应用中由激发光强度波动、测试环境条件波动等引起的误差的校正。该有机纳米光学传感器在

672 nm 处有一个红色的磷光发射带,该发射带来自 PdTFPP 磷光染料,且信号强度随葡萄糖浓度升高而增强,可作为响应峰探测葡萄糖的浓度信息。以上两峰相隔较远,几乎无光谱交叠,可构成葡萄糖传感的内参比体系。当传感器所处环境中的葡萄糖浓度发生变化时,因葡萄糖氧化酶催化作用引起的氧浓度就会发生变化,672 nm 处的磷光信号会随葡萄糖浓度增加而增强,而 490 nm 处的荧光信号保持不变。这一光谱结果表明该传感器具有高灵敏度的特点。时间相关的发光光谱展示了传感器对葡萄糖的响应过程,随着不同浓度葡萄糖溶液的加入,葡萄糖氧化酶的催化反应开始进行,可观察到 672 nm 处的磷光信号强度随反应进行而逐渐增强,在 10 min 时具有较好的传感区分,如图 3(b)所示。由图 3(c)所示的传感器的发光峰强度比值($I_{672\text{ nm}}/I_{490\text{ nm}}$)与葡萄糖浓度的对应关系可知该传感器在 0~20 mmol/L 血糖浓度范围内表现良好($R^2 > 0.99$)。

良好的生物相容性是传感器用于细胞成像、动物实验及人体临床应用的前提条件。进一步,将发光纳

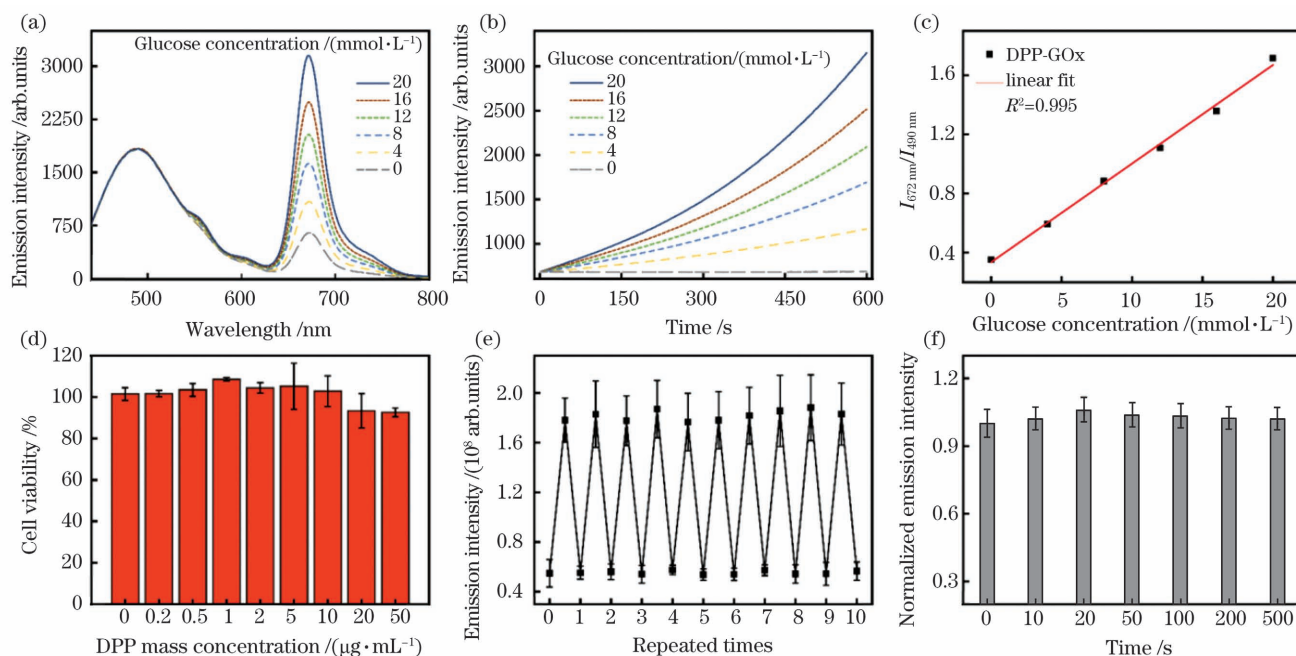


图 3 有机纳米光学传感器 DPP-GOx 的光谱学特性表征及生物相容性测试。(a)不同葡萄糖浓度(0~20 mmol/L)下有机纳米光学传感器的发射光谱;(b)不同葡萄糖浓度(0~20 mmol/L)下有机纳米光学传感器在 672 nm 处磷光强度的时间响应曲线;(c)有机纳米光学传感器在 672 nm 与 490 nm 处发光峰强度比值与葡萄糖浓度(0~20 mmol/L)的对应关系;(d)人类乳腺癌细胞与不同浓度 DPP 粒子共同孵育 24 h 后的细胞存活率;(e)依次置于 PBS 溶液与葡萄糖溶液(20 mmol/L)后,包埋于聚丙烯酰胺水凝胶中的传感器的发光强度测试结果;(f)在 20 mmol/L H_2O_2 环境中经过不同时长紫外光照射后,有机纳米光学传感器的归一化发光强度

Fig. 3 Spectroscopic characterization and biocompatibility of organic nanoparticle transducer DPP-GOx. (a) Emission spectra of organic nanoparticle transducer at different glucose concentrations (0–20 mmol/L); (b) phosphorescence intensity (at 672 nm) of organic nanoparticle transducer versus time under different glucose concentrations (0–20 mmol/L); (c) emission peak intensity ratio ($I_{672\text{ nm}}/I_{490\text{ nm}}$) of organic nanoparticle transducer as a function of glucose concentrations (0–20 mmol/L); (d) cell viability of MCF7 cells incubated with DPP with different concentrations for 24 h; (e) repeated luminescence intensity test of polyacrylamide hydrogel loaded with organic nanoparticle transducer in PBS and glucose solution (20 mmol/L); (f) normalized luminescence intensity of organic nanoparticle transducer incubated with H_2O_2 (20 mmol/L) under UV excitation for different time

米粒子 DPP 与人类乳腺癌细胞共培养,然后测试 DPP 的细胞毒性。与不同浓度的发光纳米粒子 DPP 共培养 24 h 后,测试细胞存活率。结果表明,与发光纳米粒子 DPP 共孵育并未引起明显的细胞存活率变化,如图 3(d)所示。这表明该发光纳米粒子 DPP 具有良好的生物相容性。将传感器 DPP-GOx 包埋于聚丙烯酰胺水凝胶中,并将其依次置于 PBS 环境与葡萄糖环境中,测试其葡萄糖响应表现的可重复性。如图 3(e)所示,该传感器的葡萄糖响应能力在 10 次重复测试后未见明显下降,表明该传感器具有良好的测试稳定性。将该传感器置于 H_2O_2 环境中,在不同时长的紫外光照射后测试其发光强度。结果表明,溶液中的 H_2O_2 及其在紫外光照下分解产生的羟基自由基未对传感器

的发光表现产生明显影响,如图 3(f)所示。这说明该传感器具有良好的发光稳定性及化学稳定性。该传感器对葡萄糖检测的高灵敏度、高响应速度、良好的生物相容性和测试稳定性以及高发光稳定性为进一步的细胞成像检测与动物血糖浓度检测奠定了基础。

3.3 细胞内葡萄糖传感

该传感器可用于细胞内葡萄糖代谢水平的成像检测。采用无糖培养基进行人类乳腺癌细胞培养,并将该传感器与细胞共培养 12 h 后进行成像。相较于未与传感器共培养的对照组,可观察到共培养细胞内明显的发光信号,表明该传感器已成功被人类乳腺癌细胞内吞,并保持有发光特性,如图 4(a)、(b)所示。进一步向细胞培养基中引入葡萄糖溶液,使培养基中葡

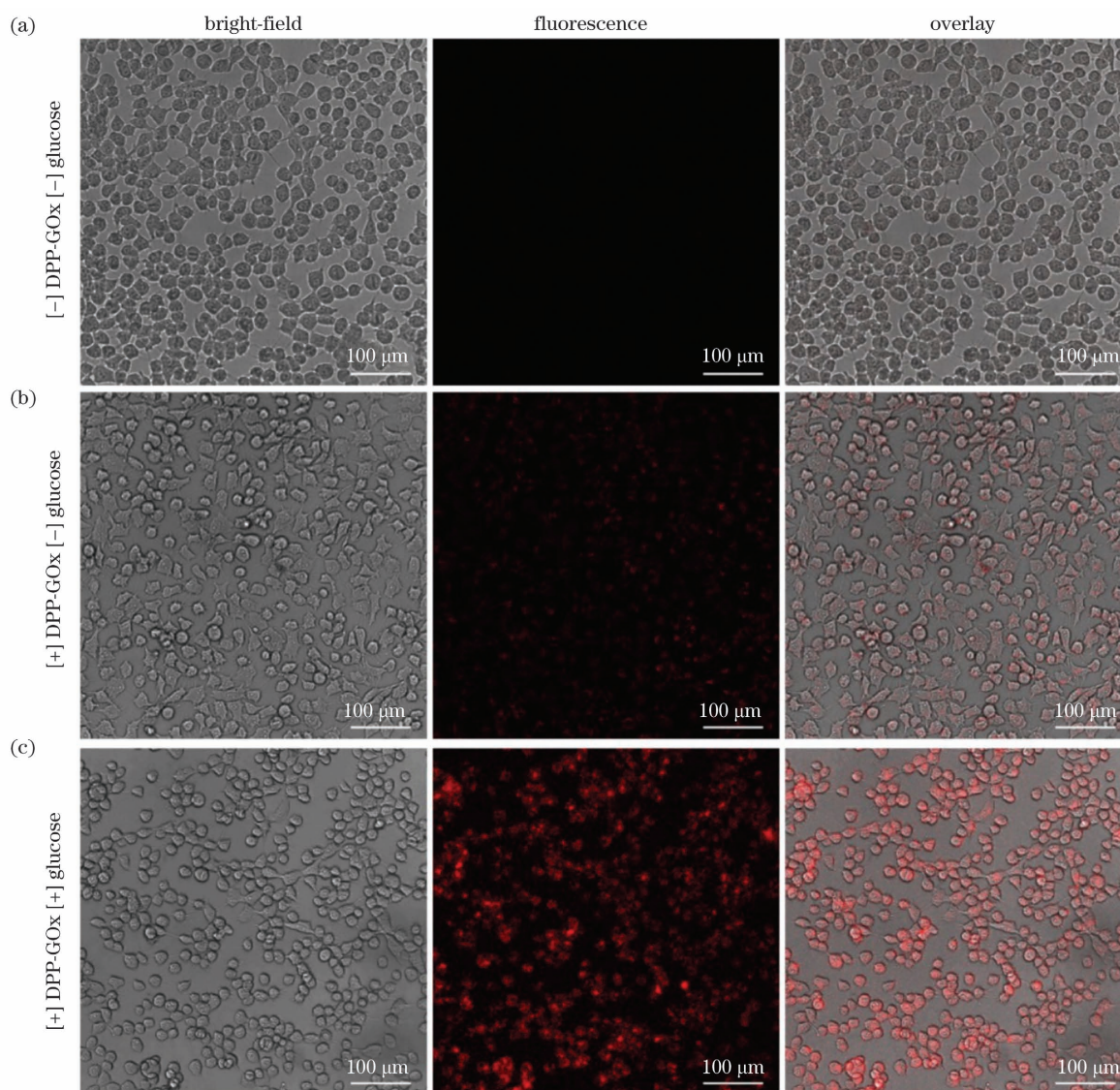


图 4 有机纳米光学传感器 DPP-GOx 对细胞内葡萄糖水平的检测。(a)在无糖培养基中未与传感器 DPP-GOx 共孵育的人类乳腺癌细胞图像(作对照实验组);(b)与传感器 DPP-GOx 共孵育 12 h 的人类乳腺癌细胞图像;(c)在无糖培养基与传感器 DPP-GOx 共孵育 12 h 并补充葡萄糖溶液的人类乳腺癌细胞图像

Fig. 4 Intracellular glucose level detection based on organic nanoparticle transducer. (a) MCF-7 cells incubated without DPP-GOx transducer in sugar-free medium as the control group; (b) MCF-7 cells incubated with DPP-GOx transducer in sugar-free medium for 12 h; (c) MCF-7 cells incubated with DPP-GOx transducer in sugar-free medium supplemented with glucose solution

葡萄糖的终浓度为 20 mmol/L, 继续培养 4 h 后进行成像。引入葡萄糖后可观察到明亮的发光信号, 如图 4 (c) 所示, 这表明传感器被细胞内吞后可用于检测细胞内的葡萄糖水平。该传感器具有高灵敏度以及良好的生物相容性, 可用于细胞内葡萄糖水平的检测, 具有追踪细胞内代谢水平的潜力。

3.4 活体动物皮下葡萄糖监测

该传感器可用于生物体内血糖信息的检测。通过皮下注射的方式将传感器植入到小鼠体内, 通过采集发光图像和分析传感器的发光强度变化实现对血糖信息的检测。小鼠皮下植入该有机纳米光学传感器后, 未观察到红肿等炎症反应。如图 5(a) 所示, 传感器被

植入到小鼠右侧下背部。由于发光纳米粒子具有高发光亮度, 植入皮下的传感器光学信号可经由皮肤被探测到, 为血糖信息的经皮检测提供了前提条件。通过腹腔注射葡萄糖溶液将小鼠血糖浓度由正常血糖水平上升至高血糖水平时, 可观察到传感器的信号强度随之增强, 如图 5(b) 所示。计算得到 $R^2 = 0.98$, 说明该传感器具有高准确性的葡萄糖传感特性。通过腹腔注射 PBS 进行对照实验, 小鼠血糖浓度与皮下传感器的信号强度基本保持不变, 如图 5(c)、(d) 所示。上述实验结果表明, 本团队制备的有机纳米光学传感器可用于检测细胞内和动物体内葡萄糖浓度, 具有灵敏和快速的光学响应, 为发展新型连续血糖监测设备提供了有益参考。

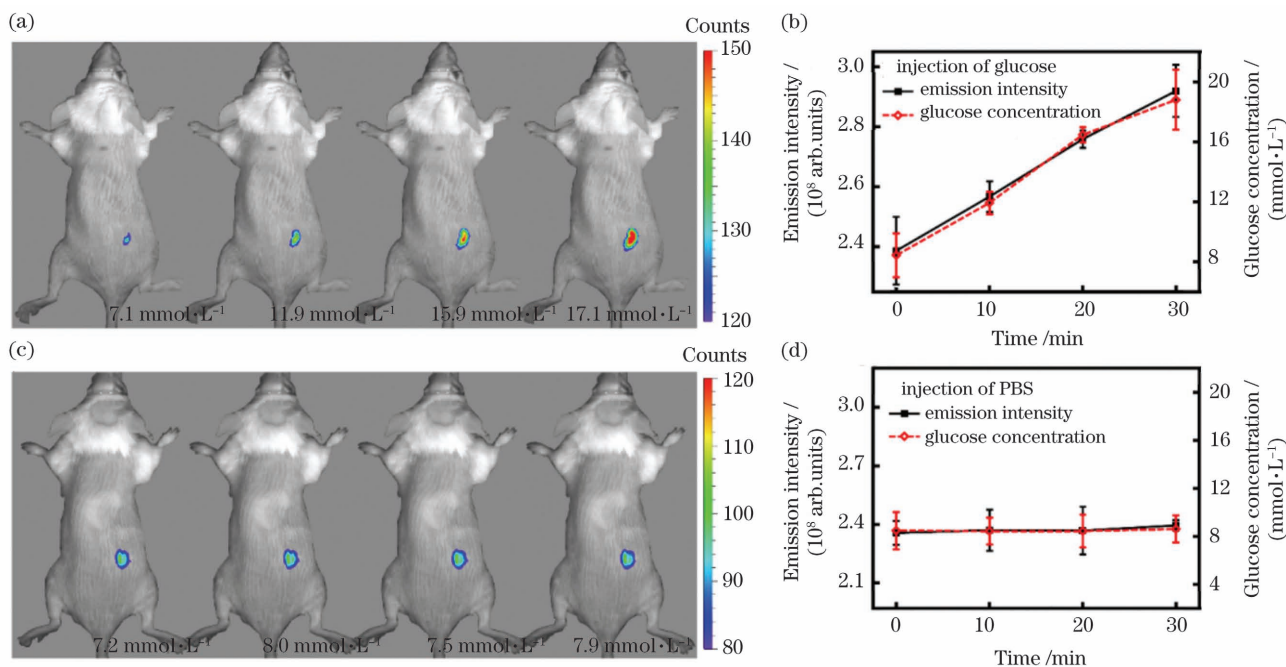


图 5 有机纳米光学传感器 DPP-GOx 对在体血糖浓度的检测。(a) 皮下植入有机纳米光学传感器并在腹腔注射葡萄糖进行升高血糖处理后的小鼠的发光图像; (b) 腹腔注射葡萄糖升高血糖后, 有机纳米光学传感器的发光强度随血糖浓度的增加而增强; (c) 皮下植入有机纳米光学传感器并在腹腔注射 PBS 后的小鼠的发光图像; (d) 腹腔注射 PBS 后, 有机纳米光学传感器的发光强度与血糖浓度保持不变

Fig. 5 *In vivo* glucose concentration monitoring by organic nanoparticle transducer DPP-GOx. (a) Luminescent images of mice implanted with DPP-GOx transducer after intraperitoneal injection of glucose solution; (b) luminescent intensity of implanted DPP-GOx transducer enhanced with the elevated blood glucose concentrations; (c) luminescent images of mice implanted with DPP-GOx transducer after intraperitoneal injection of PBS; (d) luminescent intensity of implanted DPP-GOx transducer and blood glucose concentration remain unchanged

4 结 论

本团队首先利用可见光激发的 DPBF 荧光分子、氧敏感磷光染料 PdTFPP 和两亲性聚合物 PSMA 合成了具有氧敏感特性的发光纳米粒子材料 DPP; 然后通过生物偶联的方式将葡萄糖氧化酶修饰于发光纳米粒子 DPP 表面, 构建了具有可见光激发特性的有机纳米光学传感器 DPP-GOx; 最后验证了该类传感器在细胞内葡萄糖浓度检测与在体血糖浓度监测中的性能。实验结果显示, 该类传感器可用于构建基于生物发光信号的连续血糖监测系统。相较于前期研究, 该传感

器使用可见光作为激发光源, 避免了紫外光激发造成的辐射损伤, 在高频率长时段的信号采集应用中具有巨大潜力。为了推进基于光学信号的连续血糖监测系统的实际使用, 探索高生物相容性的传感器载体, 增强长期在体植入后传感器的稳定性等仍然需要进一步研究。

参 考 文 献

- [1] Gregg E W, Sattar N, Ali M K. The changing face of diabetes complications[J]. *The Lancet Diabetes & Endocrinology*, 2016, 4(6): 537-547.
- [2] Bommer C, Sagalova V, Heesemann E, et al. Global economic burden of diabetes in adults: projections from 2015 to 2030[J].

- Diabetes Care, 2018, 41(5): 963-970.
- [3] Danne T, Nimri R, Battelino T, et al. International consensus on use of continuous glucose monitoring [J]. Diabetes Care, 2017, 40(12): 1631-1640.
- [4] Edelman S V, Argento N B, Pettus J, et al. Clinical implications of real-time and intermittently scanned continuous glucose monitoring [J]. Diabetes Care, 2018, 41(11): 2265-2274.
- [5] Lee I, Probst D, Klonoff D, et al. Continuous glucose monitoring systems—current status and future perspectives of the flagship technologies in biosensor research [J]. Biosensors and Bioelectronics, 2021, 181: 113054.
- [6] Wang J. Electrochemical glucose biosensors [J]. Chemical Reviews, 2008, 108(2): 814-825.
- [7] Teymourian H, Barfidokht A, Wang J. Electrochemical glucose sensors in diabetes management: an updated review (2010–2020) [J]. Chemical Society Reviews, 2020, 49(21): 7671-7709.
- [8] Nightingale A M, Leong C L, Burnish R A, et al. Monitoring biomolecule concentrations in tissue using a wearable droplet microfluidic-based sensor [J]. Nature Communications, 2019, 10: 2741.
- [9] Shibata H, Heo Y J, Okitsu T, et al. Injectable hydrogel microbeads for fluorescence-based *in vivo* continuous glucose monitoring [J]. Proceedings of the National Academy of Sciences of the United States of America, 2010, 107(42): 17894-17898.
- [10] Heo Y J, Shibata H, Okitsu T, et al. Long-term *in vivo* glucose monitoring using fluorescent hydrogel fibers [J]. Proceedings of the National Academy of Sciences of the United States of America, 2011, 108(33): 13399-13403.
- [11] Wu M X, Zhang Y J, Liu Q, et al. A smart hydrogel system for visual detection of glucose [J]. Biosensors and Bioelectronics, 2019, 142: 111547.
- [12] 黄珊, 朱书缘, 赵蒙蒙, 等. 组织模型中葡萄糖的近红外光谱特性 [J]. 激光与光电子学进展, 2020, 57(15): 153006.
Huang S, Zhu S Y, Zhao M M, et al. Near-infrared spectroscopy characteristics of glucose in tissue phantom [J]. Laser & Optoelectronics Progress, 2020, 57(15): 153006.
- [13] 李芬, 赵跃进, 孔令琴, 等. 基于可见光图像的无创血糖测量仿体实验验证 [J]. 光学学报, 2020, 40(6): 0636001.
Li F, Zhao Y J, Kong L Q, et al. Phantom experimental verification of non-invasive blood glucose measurement based on visible image [J]. Acta Optica Sinica, 2020, 40(6): 0636001.
- [14] 李娇, 李帅, 陈冀景, 等. 非接触光声成像研究进展及其在生物医学上的应用 [J]. 中国激光, 2021, 48(19): 1918005.
Li J, Li S, Chen J J, et al. Progress and biomedical application of non-contact photoacoustic imaging [J]. Chinese Journal of Lasers, 2021, 48(19): 1918005.
- [15] Wu C F, Chiu D T. Highly fluorescent semiconducting polymer dots for biology and medicine [J]. Angewandte Chemie (International Ed. in English), 2013, 52(11): 3086-3109.
- [16] Wu C F, Bull B, Christensen K, et al. Ratiometric single-nanoparticle oxygen sensors for biological imaging [J]. Angewandte Chemie (International Ed. in English), 2009, 48(15): 2741-2745.
- [17] Chen S J, Wang H, Hong Y N, et al. Fabrication of fluorescent nanoparticles based on AIE luminogens (AIE dots) and their applications in bioimaging [J]. Materials Horizons, 2016, 3(4): 283-293.
- [18] Reisch A, Klymchenko A S. Fluorescent polymer nanoparticles based on dyes: seeking brighter tools for bioimaging [J]. Small, 2016, 12(15): 1968-1992.
- [19] Sun K, Tang Y, Li Q, et al. *In vivo* dynamic monitoring of small molecules with implantable polymer-dot transducer [J]. ACS Nano, 2016, 10(7): 6769-6781.
- [20] Sun K, Yang Y K, Zhou H, et al. Ultrabright polymer-dot transducer enabled wireless glucose monitoring via a smartphone [J]. ACS Nano, 2018, 12(6): 5176-5184.
- [21] Sun K, Ding Z Y, Zhang J C, et al. Enhancing the long-term stability of a polymer dot glucose transducer by using an enzymatic cascade reaction system [J]. Advanced Healthcare Materials, 2021, 10(4): e2001019.
- [22] Sun K, Liu S Y, Liu J, et al. Improving the accuracy of pdot-based continuous glucose monitoring by using external ratiometric calibration [J]. Analytical Chemistry, 2021, 93(4): 2359-2366.
- [23] Biniek K, Levi K, Dauskardt R H. Solar UV radiation reduces the barrier function of human skin [J]. Proceedings of the National Academy of Sciences of the United States of America, 2012, 109(42): 17111-17116.
- [24] Fang X F, Chen X Z, Li R Q, et al. Multicolor photo-crosslinkable AIEgens toward compact nanodots for subcellular imaging and STED nanoscopy [J]. Small, 2017, 13(41): 1702128.
- [25] Wu C F, Szymanski C, McNeill J. Preparation and encapsulation of highly fluorescent conjugated polymer nanoparticles [J]. Langmuir: the ACS Journal of Surfaces and Colloids, 2006, 22(7): 2956-2960.
- [26] Wu C F, Peng H S, Jiang Y F, et al. Energy transfer mediated fluorescence from blended conjugated polymer nanoparticles [J]. The Journal of Physical Chemistry B, 2006, 110(29): 14148-14154.

Quantitative Imaging of Blood Glucose Concentration Using Organic Nanoparticle Transducer

Liu Jing^{1,2}, Fang Xiaofeng², Yuan Zhen¹, Wu Changfeng^{2*}

¹Cancer Center, Faculty of Health Science, University of Macau, Macau SAR 999078, China;

²Department of Biomedical Engineering, College of Engineering, Southern University of Science and Technology, Shenzhen 518055, Guangdong, China

Abstract

Objective Diabetes mellitus is a chronic and noncommunicable disease with complications in the retina, heart, kidney, and neural system. The effective monitoring of blood glucose level is crucial in the prevention, diagnosis, and management of diabetes. Compared with single-point detection, a continuous glucose monitoring system can track the blood glucose fluctuation and help in predicting the trend of blood glucose change. Recently, various continuous glucose

monitoring systems have been developed. The most widely used monitoring modality is electrochemical sensors, which collect glucose information in the interstitial fluid using an implanted enzyme-immobilized electrode. However, electrochemical sensors have some issues, including the limited glucose monitoring time and the risk of infection. Conversely, transdermal detection-based optical sensors exhibit prolonged service time and decreased risk of infection. Luminescent nanoparticles have shown great potential in biological applications because of their high brightness, high photostability, and good biocompatibility. Here, we developed a continuous glucose monitoring system based on a visible-light-excited nanoparticle transducer. We experimentally demonstrated that the nanoparticle transducer is promising for sensitive glucose detection. The visible-light-excited transducer shows potential in long-term and high-frequency monitoring in practical applications with reduced side effects compared with ultraviolet radiation.

Methods The nanoparticles were prepared using a visible-light-excited fluorescent molecule and the oxygen-sensitive phosphorescent dye via the reprecipitation method. The resulting nanoparticles were characterized via UV-Vis absorption spectra, transition electron microscopy (TEM), and dynamic light scattering (DLS) measurements. The glucose-sensitive nanoparticle transducer was formed by modifying glucose oxidase onto the surface of nanoparticles via EDC-catalyzed bioconjugation. The successful bioconjugation of oxygen-consuming enzyme onto the nanoparticle was characterized by the change in hydrodynamic diameters and zeta-potentials. The biocompatibility of the nanoparticles was characterized through cytotoxicity experiment. The glucose sensitivity of the nanoparticle transducer was examined by measuring the emission spectra under different glucose concentrations (0–20 mmol/L). The intracellular glucose sensing of the nanoparticle transducer was performed on MCF-7 cells. The MCF-7 cells were incubated with the nanoparticle transducer first in a sugar-free medium. Additional glucose solution was introduced with the final concentrations at 20 mmol/L. The luminescence images under different glucose concentrations (0 and 20 mmol/L) were captured.

We investigated the *in vivo* glucose monitoring performance of the nanoparticle transducer. The nanoparticle-GOx transducer (50 $\mu\text{g}/\text{mL}$) was subcutaneously implanted in the lower back of mice under anesthesia. The blood glucose concentrations of the mice were elevated by the intraperitoneal injection of glucose solutions (1 mol/L, in Milli-Q water). Subsequently, blood samples were collected from the tail of mice, and the blood glucose concentrations were tested using a commercial glucometer. Using a small animal biophotonic imaging system, the luminescence images of the subcutaneously implanted nanoparticle-GOx transducer were collected. The luminescence intensity of the implanted nanoparticle transducer was measured and compared with blood glucose concentrations. The mice with the intraperitoneal injection of PBS were adopted as the control group.

Results and Discussions The oxygen-sensitive nanoparticle comprises a fluorescent molecule DPBF, an oxygen-sensitive phosphorescent dye PdTFPP, and a functional polymer PSMA. The resulting nanoparticles have a hydrodynamic diameter of 18 nm, as indicated by the TEM and DLS results. The successful bioconjugation of glucose oxidase onto the nanoparticle surface was characterized by the increased hydrodynamic diameters and zeta-potentials. According to the spectroscopic experiments, the phosphorescence intensity (~ 672 nm) of the nanoparticle-GOx transducer increased as the glucose concentration increased, whereas the fluorescence intensity (~ 490 nm) remained unchanged. The designed ratiometric sensing system can help in eliminating the luminescence fluctuations caused by the variation in excitation intensity and environmental conditions. The nanoparticle-GOx transducers exhibited a fast response time to distinguish different glucose concentrations. The luminescence spectra of the nanoparticle-GOx transducers under different glucose concentrations were measured within 10 min after adding glucose to the solution. A good correlation was exhibited between the luminescence intensity of the nanoparticle-GOx transducers and glucose concentrations.

The cell viability of the MCF-7 cells did not change considerably after incubating with the nanoparticles at different concentrations. The results indicated that the nanoparticles are biocompatible for the following intracellular glucose sensing experiments and *in vivo* glucose monitoring experiments. The nanoparticle-GOx transducer exhibited a reversible response to glucose, and the monitoring performance remained unchanged for more than 10 repetitive tests. The nanoparticle-GOx transducer exhibited excellent photostability against hydrogen peroxide and free radicals. The reversible response and excellent photostability enabled the stable and long-term continuous glucose monitoring. After adding glucose, the luminescence intensity of the internalized nanoparticle transducers by the cells was obviously enhanced, indicating that the nanoparticle transducer has the potential for intracellular glucose sensing. For *in vivo* glucose monitoring, we collected the luminescence images of subcutaneously implanted nanoparticle transducers. The transdermal detection of the nanoparticle transducers was achieved because of its high brightness. After the intraperitoneal injection of glucose solution, the luminescence intensity of the subcutaneously implanted transducers increased with the increased blood glucose concentrations, whereas in the control group, the luminescence intensity and blood glucose concentrations remain unchanged after the intraperitoneal injection of PBS. These results indicate that the luminescent nanoparticle transducers are promising for *in vivo* continuous glucose sensing.

Conclusions We developed a continuous glucose monitoring system based on a visible-light-excited luminescent nanoparticle transducer. The nanoparticle transducer can be used for the transdermal detection of blood glucose because of its high luminescence brightness. We demonstrated *in vitro* cellular glucose sensing and *in vivo* glucose monitoring in animal models. With the ratiometric sensing system, the signal fluctuations caused by the variation in excitation intensity and environmental conditions would be eliminated. The visible-light-excited transducer can also avoid the side effects induced by ultraviolet radiation, indicating the potential for long-term and high-frequency monitoring in practical applications.

Key words bio-optics; sensors; nanoparticle sensor; biosensors; blood glucose monitoring